

Effect of Chain Length and Topological Constraints on Segmental Relaxation in Cyclic PDMS

Valeria Arrighi,^{*,†} Simona Gagliardi,[†] Fabio Ganazzoli,[‡] Julia S. Higgins,[§] Giuseppina Raffaini,[‡] Jeerachada Tanchawanich,[†] Jenny Taylor,[†] and Mark T. F. Telling^{||,⊥}

[†]Institute of Chemical Sciences, School of Engineering and Physical Science, Heriot-Watt University, Edinburgh EH14 4AS, United Kingdom

[‡]Dipartimento di Chimica, Materiali e Ingegneria Chimica "Giulio Natta", Politecnico di Milano, via L. Mancinelli 7, 20131 Milano, Italy

[§]Chemical Engineering Department, Imperial College London, South Kensington Campus, London SW7 2AZ, United Kingdom

^{||}ISIS, Rutherford Appleton Laboratory, Chilton, Didcot OX11 0QX, United Kingdom

[⊥]Department of Materials, University of Oxford, Parks Road, Oxford OX1 3PH, United Kingdom

ABSTRACT: We present a detailed investigation of local dynamics of linear and cyclic poly(dimethylsiloxane) (PDMS) covering a wide range of molar masses. To aid interpretation of the experimental data, QENS measurements in the time scale from 2 to 200 ps and at $Q = 0.3$ to 1.8 \AA^{-1} are complemented by theoretical calculations. These make use of a methodology developed by us elsewhere applicable to both simple chain models and real chains and applied here, for the first time, to cyclic PDMS. Analysis of the incoherent dynamic structure factor at $T < T_m$ shows that the rotational motion of the methyl groups is unaffected by polymer topology. At higher temperatures, the QENS data are described by a model that consists of two dynamic contributions: methyl group rotation and segmental motion, the latter described by a stretched exponential function. Relaxation times of both linear and cyclic PDMS increase with increasing molar mass.

Several features predicted by theory are also reproduced by the experimental data. We show, unambiguously, that rings have higher relaxation times for the segmental motion compared to linear chains of the same number of monomer units. Theoretical calculations support the idea that such slowing down of local dynamics is due to the topological constraint imposed by the ring closure, a constraint which becomes negligible for very large molar masses. Our calculations suggest that due to its albeit small conformational rigidity, cyclic PDMS undergoes an additional constraint which further increases the relaxation time, producing a shallow maximum for $N \approx 50$ repeat units. A similar feature is also observed in the experimental QENS data. Values of activation energy, E_a , are derived from analysis of the temperature dependence of the quasi-elastic broadening and are found to be in agreement with viscosity measurements reported in the literature. Although the pronounced molar mass dependence of E_a for linear PDMS is certainly linked to the presence of mobile chain ends, for the cyclic polymers the behavior appears to be more complex than anticipated.

1. INTRODUCTION

Cyclic polymers differ from linear chains by one single bond that links the chain ends. This apparently trivial topological constraint has a profound effect on many polymer properties.¹ For example, it has been shown to influence crystallization,^{2–4} thermal properties such as heat capacity⁵ and glass transition,^{4,6–9} bulk viscosity,^{10–12} and diffusion coefficients.^{13–16}

Early theoretical studies focused on the effect of polymer topology on conformation and radii of gyration,^{17–20} glass transition, and dynamics.²¹ Extensive work has also been carried out using computer simulations.^{22–29} Experiments on well-characterized cyclic molecules have made it possible to confirm theoretical predictions of chain dimension in solution^{17,19,30–35}

and in bulk,^{36–39} leading to a good understanding of their structural properties. Recently, good agreement between theory and experiments was reported by us for cyclic poly(dimethylsiloxane)s (PDMS) in the undiluted state. Our results showed that highly flexible cyclic polymers in the melt adopt an even more compact conformation than that of unperturbed rings, leading to that $R_g \propto M_w^{0.4}$.^{36,37}

In this work we make a comparison between linear and cyclic PDMS dynamics. Although macroscopic properties such as bulk

viscosity^{10–12} and diffusion coefficients^{13–16} have been well documented in the literature, fewer studies have addressed microscopic behavior. Here, using quasi-elastic neutron scattering (QENS), we aim to provide a microscopic insight into the different dynamic behavior of linear and cyclic molecules, within length scales that are sensitive to molecular structure.

Experimental and theoretical studies of melt dynamics have focused on the extent to which chain ends, or better the absence of, affect the dynamic behavior of a polymer.²¹ Chain motion in a dense solution or melt of entangled linear or branched chains is well understood in terms of the reptation model.^{40–43} However, the concept of reptation is strictly correlated to the existence of chain ends, and for this reason this type of motion should be strongly suppressed in nonlinear polymers such as stars or closed ring molecules.^{21,44}

Generally, theoretical predictions of significant differences between the melt dynamics of linear and cyclic polymers have not been fully supported by experiments. Early viscoelastic measurements of cyclic polystyrene produced contradictory results, particularly with regard to the molecular weight dependence of the viscosity.^{32,45,46} By carrying out measurements of the recoverable compliance for several cyclic polystyrene (PS) fractions from different sources, McKenna et al. were able to demonstrate that discrepancies between results were primarily due to the presence of linear chains and/or formation of knots.⁴⁷ As shown by these authors, the molecular weight dependence of the zero-shear rate viscosities in the molten state shows similar features for the cyclics and the linear chains. In the case of PS, over the entire range of molecular weights (above $M_w = 11000 \text{ g mol}^{-1}$) and at constant $T - T_g$, the

rings exhibit a lower viscosity compared to values measured for linear chains of the same M_w . At relatively low molecular weights the ratio between the viscosity of linear chains and rings was found to be ≈ 2 , as expected from differences between their radii of gyration (the ratio between the squared radii of gyration of linear chains and rings should be equal to 2).^{17–20} A similar result was reported by Bras et al.³⁸ for low molecular weight linear and cyclic poly(ethylene oxide) (PEO). However, for PEO, linear and ring polymers were reported to have the same activation energy, indicating that the temperature dependence of the segmental friction does not depend on polymer topology. The authors noted that this result is consistent with an earlier observation of the same shift factors for entangled linear and ring polymers.⁴⁸

On the basis of the rheological data, diffusion should be faster for rings than linear chains. This is supported by computer simulations which indicate that topological interactions greatly influence melt dynamics leading to faster diffusion for melts of rings and shorter relaxation times compared to linear chains of equal mass.^{22–29} Interdiffusion experiments of bilayers consisting of cyclic PS and deuterated cyclic PS have shown faster mutual diffusion compared to equivalent bilayers of linear chains, providing experimental support for simulations.⁴⁹ In addition to this, qualitative agreement between atomistic MD simulations and neutron spin-echo (NSE) measurements has been reported for PEO, with diffusion coefficients that are faster by a factor of 2 for the rings.³⁸

Perhaps one of the most surprising observations is that for both cyclics and linear molecules the molecular weight dependence of the viscosity exhibits two power law regimes. Because the change in power law dependence has been attributed to a transition from unentangled to entangled behavior,

it is somewhat unexpected for cyclics. In a recent review, Richter et al.⁵⁰ compared viscosity data at the same distance from the glass transition temperature, i.e., at iso-frictional conditions, for a number of systems including polystyrene,^{47,33} polybutadiene,⁵¹ and PEO.⁵² In all cases, two regimes can be identified: (a) at low molecular weights, for unentangled chains, the ratio between the viscosity of linear chains and rings, η_l/η_r , is constant and equal to 2, but (b) above the entanglement molecular weight it increases above this value depending on the number of entanglements. As shown by recent work on high molecular weight cyclic polymers, understanding the relaxation mechanisms of melts of rings is challenging and requires high molecular weight cyclics, free from contamination.^{53,50,54}

In this paper, following previous studies including our own work,^{55–58} we present a systematic investigation of the influence of topology on local chain motion by comparing QENS data of linear and cyclic PDMS. As reported in our paper, QENS is used to observe length scales up to a few statistical segment lengths. In this case, molecular motion (very local motion of side chains, monomers, or short segments of the polymer chains) is largely determined by intramolecular potentials and, due to the limited length scale of observation, independent of the nature of the entangled or unentangled chains. Our QENS data differ considerably from the neutron spin-echo (NSE)₅₀ coherent scattering results recently reported in the literature.⁵⁰ This is because spin-echo at small angles is designed to explore length scales close or above to the entanglement length where reptation dominates. Thus, NSE data are crucially dependent on interchain interactions such as entanglements. Here we focus on relatively small molecular weight PDMS samples, largely below the entanglement molecular weight (reported to be equal to 12293 g mol^{-1} by Fetter et al.⁵⁹ but much higher, $M_e = 34500 \text{ g mol}^{-1}$, according to data of Dvornic et al.⁶⁰).

The local dynamics of PDMS has been investigated extensively by neutron scattering^{57,58,61} and other experimental techniques such as dielectric spectroscopy^{62–65} as well as simulations.⁶⁶ Most of these studies have dealt with linear high molecular weight chains, and there is little in the literature on the comparison between cyclic and linear PDMS dynamics, except for QENS measurements reported by Allen et al.^{56,67} For samples with degree of polymerization < 20 (equivalent to $M_n \leq 1500 \text{ g mol}^{-1}$), these authors reported effective diffusion coefficients (extracted from the quasi-elastic broadening) which were greater for linear chains compared to rings. This indicated that short linear PDMS chains are faster than the small rings, the difference becoming more pronounced with decreasing molecular weight.

The QENS results of Allen et al.^{56,67} find support in the bulk viscosity data of Semlyen and co-workers,^{10–12} indicating that the viscosity of cyclic PDMS is higher than that of linear PDMS at comparably low molecular weights, but the opposite behavior is observed in the high molecular weight region. The existence of a crossover region in the M_w dependence of the viscosity could not be simply attributed to chain end effects and was still evident even after scaling at constant segmental mobility. Semlyen et al. argued that configurational restrictions in the ring molecules would be responsible for a reduction in segmental mobility, resulting in higher viscosity at low molecular weight.^{10–12}

The main motivation of the work presented in the following sections is to characterize the molecular weight dependence of the local dynamics of relatively short chains and small rings. Compared to previous measurements, we cover a wide range of molar masses, and we present a detailed analysis of the

incoherent dynamic structure factor, including temperature and Q dependence. The experimental data are supplemented by theoretical calculations using a methodology developed by us elsewhere applicable to both simple chain models and real chains.⁵⁵ The same methodology is extended here, for the first time, to cyclic PDMS.

2. EXPERIMENTAL METHODS AND THEORETICAL APPROACH

2.1. Materials. Table 1 gives a list of samples used for the neutron scattering measurements. The linear PDMS samples, with trimethylsilo-

Table 1. Molar Mass and Thermal Transitions of Linear (L) and Cyclic (C) PDMS

code	η_k^a (cSt)	M_n (g mol ⁻¹)	M_w/M_n	T_g (K)	T_m (K)
L162	0.65	162		110	210
L237	1	237		125	190
L550	3.0	550		136	
L1400		1430 ^b	1.02	145	
L2000	20	2000		148	
L3780	50	3780		149	220, 235
L9430	200	9430		149	220, 235
C370		370		165	227
C445		445		157	270
C1200		1218 ^b	1.08	152	
C2700		2675 ^b	1.03	151	
C19000		19000 ^c		150	229, 239

^aKinematic viscosity in cSt, as reported by manufacturer at 25 °C. ^bSupplied and characterized by Dr. J. A. Semlyen and Prof. P. Griffiths. ^cAverage number of repeat units, $N_n = 257$.

xy terminal groups, are commercial materials from Dow Corning Ltd. The molecular weights of these linear samples, except for L162 and L237, were obtained from the manufacturer and are consistent with values reported by Cowie et al. for silicone fluids of comparable viscosity.⁴⁸ Cyclic PDMS samples were provided by Dr. J. A. Semlyen and Prof. P. Griffiths except for C370 and C445 that were purchased from Sigma-Aldrich. L1400 was also kindly supplied and characterized by Dr. J. A. Semlyen and co-workers. Number-average molar masses, M_n , and polydispersities (M_w/M_n) of the cyclic siloxanes as well as values for L1400 were obtained by Semlyen and co-workers using gel permeation chromatography calibrated using standard siloxane samples.

2.2. Thermal Properties: T_g and Crystallization. To determine the lower temperature at which QENS experiments can be performed, the melting temperatures, T_m , of the linear and cyclic samples were measured using a TA Instruments differential scanning calorimeter (DSC 2010) with both heat flow and temperature scales calibrated against indium metal. DSC measurements were performed under a nitrogen flow at a heating rate of 10 °C min⁻¹. T_m values for semicrystalline samples are reported in Table 1. Our results are in good agreement with the work of Clarson et al.,⁴ who demonstrated that cyclic siloxanes with number-average repeat units, N_n , in the range $12 \leq N_n \leq 40$ ($890 \leq M_n \leq 2930$) as well as linear chains with $6 \leq N_n < 21$ ($530 \leq M_n \leq 1645$) do not crystallize.

We note that for L3780, L9430, and C19000 two melting peaks were observed in the DSC trace. This characteristic feature of PDMS samples has been reported by others and attributed to melting of two different crystalline forms of the polymer.^{69,70}

The molecular weight dependence of the glass transition temperature, T_g , of both linear and cyclic PDMS has been reported in the literature.^{4,68} A linear relationship between T_g and M_n^{-1} was observed for both linear and cyclic PDMS, but while the former has a negative slope (-6.5×10^3 K g mol⁻¹) the latter displays a positive slope (3.6×10^3 K g mol⁻¹).⁴ Similar trends were determined from dielectric measurements of cyclic and linear PDMS fractions by Goodwin et al.⁶⁵

Glass transitions listed in Table 1 have been derived from the known molar mass dependence reported in the literature.^{4,68} For amorphous samples, experimental T_g values (not shown) are consistent with this trend (within 2–3 K).

As shown in Table 1, in agreement with experiments^{4,68,65} as well as theoretical predictions,⁶ for chains of similar length, the T_g of the rings is always at higher temperature compared to that of linear chains. The molecular weight dependence of T_g for cyclic PDMS was explained by Di Marzio and Guttman in terms of their configurational entropy model.⁶

2.3. Neutron Scattering Measurements. Quasi-elastic neutron scattering experiments were performed on the high energy resolution backscattering spectrometers IRIS and OSIRIS (ISIS, Rutherford Appleton Laboratory, UK) using the PG002 (offset) analyzer configuration, which gives energy resolutions (measured as fwhh) of 17.5, and 24.5 μ eV for IRIS and OSIRIS, respectively. This energy resolution affords access to a temporal range spanning ca. 2–200 ps. The energy range covered in all experiments was -0.2 to 1.0 meV, and the Q range varied from 0.5 to 1.8 \AA^{-1} . Hollow cylinders were used to contain the liquid samples during the IRIS and OSIRIS measurements. The sample's thickness was less than 0.25 mm, corresponding to a transmission of more than 90% of the incident neutron beam. At this level multiple neutron scattering effects were deemed negligible.

For each sample, at least one set of QENS data were collected at 110 deg above the respective T_g . To explore the temperature dependence of the dynamics, one of the linear siloxanes (L550) and all of the cyclic samples were measured at selected temperatures above their T_g . In addition to this, for a few cyclics, QENS spectra were recorded below the polymer T_g .

In a QENS experiments, the scattered intensity is measured as a function of both energy and momentum transfer, Q ($= (4\pi/\lambda) \sin(\theta/2)$), where λ is the neutron wavelength and θ is the scattering angle). The dynamic incoherent structure factor, $S(Q, \omega)$, is determined from time-of-flight data, after removing empty cell contributions and correcting for absorption, using standard software available at ISIS.

$S(Q, \omega)$ is related to the double differential scattering cross section, $\frac{\partial^2 \sigma}{\partial E \partial \Omega}$ which represents the probability that a neutron is scattered with energy change ΔE into the solid angle $\Delta \Omega$. For neutrons scattered incoherently

$$\left(\frac{\partial^2 \sigma}{\partial \Omega \partial E} \right)_{\text{inc}} = \frac{Nk}{k_0} \Delta b^2 S_{\text{inc}}(Q, \omega) \quad (1)$$

where N is the number of atoms, and k and k_0 represent the magnitude of the scattered and incident wave vectors ($k = 2\pi/\lambda$), respectively. The term Δb^2 depends on fluctuations of the scattering length b due to the presence of different isotopes, and it is related to the incoherent cross section ($\sigma_{\text{inc}} = 4\pi \Delta b^2$).

For PDMS, $\sigma_{\text{inc}} = 481.6$ b, which is much larger than the coherent cross section of the repeat unit, $\sigma_{\text{coh}}(\text{H}) = 28.4$ b. As a result, coherent scattering is negligible, and as stated by eq 1, the total scattering cross section is approximated to the incoherent scattering cross section, hence the subscript “inc”.

The incoherent scattering law, $S_{\text{inc}}(Q, \omega)$, is defined as the time-Fourier transform of the intermediate scattering function $I_{\text{inc}}(Q, t)$:

$$S_{\text{inc}}(Q, \omega) = \frac{1}{2\pi} \int I_{\text{inc}}(Q, t) \exp(-i\omega t) dt \quad (2)$$

which describes correlations between the positions of the same scattering nuclei at time zero and t :

$$I_{\text{inc}}(Q, t) = \frac{1}{N} \sum \langle \exp(iQ \cdot R_i(t)) \exp(-iQ \cdot R_i(0)) \rangle \quad (3)$$

where the brackets indicate a thermal average and $R_i(t)$ and $R_i(0)$ represent the position of the i th nucleus ($i = 1, 2, \dots, N$) at time t and $t = 0$, respectively. Thus, $S_{\text{inc}}(Q, \omega)$ gives dynamic information about self-correlations, rather than collective correlations, in the system under study.

Generally, the measured dynamic incoherent structure factor is a convolution of different processes

$$S_{\text{inc}}(Q, \omega) = S_{\text{inc}}^{\text{trans}}(Q, \omega) \otimes S_{\text{inc}}^{\text{rot}}(Q, \omega) \otimes S_{\text{inc}}^{\text{vib}}(Q, \omega) \quad (4)$$

i.e., vibrations (vib), rotations (rot), and translations (trans) of the scattering centers. Similarly, the intermediate scattering function can be written as the product of the different dynamic contributions:

$$I_{\text{inc}}(Q, t) = I_{\text{inc}}^{\text{trans}}(Q, t) \cdot I_{\text{inc}}^{\text{rot}}(Q, t) \cdot I_{\text{inc}}^{\text{vib}}(Q, t) \quad (5)$$

Simplifications are possible, depending on the temperature and experimental energy range.

2.4. Theoretical Calculations. The single-chain dynamics in a low molar mass melt can be described by the stochastic Langevin equation in the absence of the hydrodynamic interaction, screened by the surrounding chains. We closely follow the method described in ref 55, where we theoretically investigated the dynamics of both linear PDMS and of some coarse-grained models (freely jointed and freely rotating chains) with different degrees of local stiffness for a comparison. As a result, here we only briefly mention the basic differences due to the constraint of ring closure. We consider chains comprising N repeat units connected by harmonic springs of length l . Consequently, the linear chain and the ring have the same molar mass for a given N , but the number of connecting springs is $N - 1$ and N , respectively. In the freely jointed (FJ) model the spring comprises a few chemical repeat units and corresponds to the statistical segment devoid of any conformational correlation with the adjacent ones. On the other hand, in realistic PDMS the spring encompasses a single chemical repeat unit, or monomer, such that the length l is given by the distance between two sequential units and the conformational correlation is dictated by the preferred rotational states around the individual Si–O bonds within the RIS scheme. The elastic force matrix acting among the directly connected units is obtained as described in ref 55 and, in the absence of excluded-volume interactions (which are also screened in a melt), only depends on the topologically short-range correlations imposed by the local stiffness in PDMS and by the constraint of ring closure. Diagonalization of the elastic force matrix decouples the dynamics equations and produces both the dynamical normal modes through its eigenvectors and the (adimensional) intramolecular relaxation rates through the eigenvalues. The elements of the eigenvector matrix, V_{jp} , and the eigenvalues for the linear chain are reported in eqs 1–4 of ref 55, while in the case of the ring they are given by

$$V_{jp} = \left(\frac{1}{N}\right)^{1/2} e^{iq_p j} \quad (6)$$

where i is the imaginary unit and the Fourier coordinate q_p is

$$q_p = \frac{2\pi p}{N}, \quad p = 0, 1, 2, \dots, N - 1 \quad (7)$$

The eigenvalues are then given by μ_p/C_p , where

$$\mu_p = 4 \sin^2(q_p/2) \quad (8)$$

formally the same as in the linear chain. C_p is the generalized characteristic ratio embodying the conformational features of the chain model. For the FJ chain with no short-range correlation among the bond vectors $C_p \equiv 1$, while in real chains, within the RIS scheme C_p can be written as^{71,72}

$$C_p = \sum_{h=1}^{\nu} \alpha_h \frac{1 - g_h^2}{1 + g_h^2 - 2g_h \cos q_p} \quad (9)$$

Note that with a single term within the sum, and with $\alpha_h \equiv 1$, the above expression applies to a freely rotating chain model, with $g = -\cos \theta$, θ being the fixed “bond” angle formed by adjacent “bond” vectors. Using the RIS scheme,⁷³ the values for some real polymers, including also PDMS, are reported in ref 72, with ν in principle equal to three (i.e., the space dimensionality) times the number of rotational energy minima around a single bond. However, in practice, only 4–5 nonvanishing terms are required in the sum of eq 9, provided the chemical repeat unit is effectively treated as a whole. In this case, l is simply equal to the distance between corresponding atoms in adjacent monomers, and it is

equal to 2.9 Å as an average value for the Si...Si and O...O separation in PDMS. It should be noted that in a ring polymer the cyclic symmetry imposes a 2-fold multiplicity to the spectrum of the relaxation rate between the modes characterized by the indices p and $N - p$, as it can be seen through eqs 8 and 9. The intramolecular relaxation times τ_p , $p = 1, 2, \dots, N - 1$, are then given by

$$\tau_p = C_p / \sigma \mu_p \quad (10)$$

where σ^{-1} is the time unit

$$\sigma = 3k_B T / \zeta l^2 \quad (11)$$

with ζ being the friction coefficient of the repeat unit.

By assuming a Gaussian distribution of $\mathbf{R}_j(t) - \mathbf{R}_j(0)$, in view of the stochastic Brownian forces due to the random impulses of the surrounding molecules, the dynamic structure factor for incoherent scattering is obtained from eq 3 as

$$I_{\text{inc}}(Q, t) = \exp[-Q^2 D t] \frac{1}{N} \sum_j \exp\left[-\frac{Q^2}{6} \langle r_{jj}^2(t) \rangle\right] \quad (12)$$

where we separated the contribution of the zeroth mode with $p = 0$ that yields the diffusion coefficient D , given by the Einstein formula

$$D = k_B T / N \zeta = \sigma l^2 / 3N \quad (13)$$

from the intramolecular contribution described by the internal modes embodied by the time-dependent mean-square distance of the j th repeat unit from itself at different times

$$\langle r_{jj}^2(t) \rangle = \langle [\mathbf{R}_j(t) - \mathbf{R}_j(0)]^2 \rangle - 6Dt \quad (14)$$

irrespective of the position of the center of mass. Consequently, we have (see also ref 74)

$$\langle r_{jj}^2(t) \rangle = \frac{2l^2}{N} \sum_{p=1}^{N-1} \frac{C_p}{\mu_p} [1 - \exp(-t/\tau_p)] \quad (15)$$

Note that in view of the cyclic statistical symmetry of the ring $\langle r_{jj}^2(t) \rangle$ turns out to be independent of the j index of the repeat unit.

The calculated line shapes of $I_{\text{inc}}(Q, t)$ for the FJ chain and the PDMS rings, and for the corresponding linear chains (calculated as described in ref 55), were then fitted by the KWW stretched exponential function for relatively short times before diffusion of the center of mass sets in

$$\frac{I_{\text{inc}}(Q, t)}{I_{\text{inc}}(Q, 0)} = \exp(-(t/\tau)^\beta) \quad (16)$$

Here, both the characteristic time τ and the β exponent (<1) are assumed to depend both on Q and on N in the theoretical approach. The calculations were performed for linear chains and rings with a number of repeat units, $10 \leq N \leq 200$ (beads for the freely jointed model and monomers for real PDMS), in the range of the experimental samples choosing a Q range of $0.2 \leq Q \cdot l \leq 1.0$. From the nonlinear fit of the calculated line shape using the stretched exponential of eq 16, the correlation coefficient R turned out to be larger than 0.9999 for the FJ chain and 0.9997 for PDMS, while the mean-square residual χ^2 , normalized by the number of degrees of freedom, was smaller than 2.5×10^{-6} for the FJ chain and 3.5×10^{-5} for PDMS.

3. RESULTS

3.1. Analysis of Low-Temperature Data of Cyclic PDMS. In our previous studies,^{57,58,61} we have shown that the QENS data of PDMS melts are described by a model that consists of two dynamic contributions: methyl group rotation and segmental motion. To test whether changes to methyl group dynamics needed to be accounted for in cyclic polymers, we performed a series of measurements on a cyclic sample with $M_w = 2675 \text{ g mol}^{-1}$ (C2700) in the temperature range 158–208 K. Although this corresponds to temperatures above T_g segmental

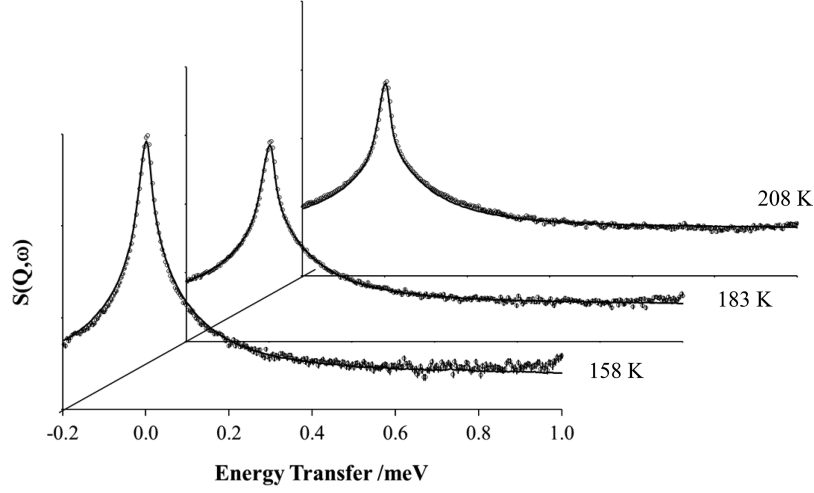


Figure 1. QENS spectra of cyclic PDMS (C2755) at 158, 183, and 208 K (from front to back) and $Q = 1.31 \text{ \AA}^{-1}$. Symbols represent experimental data and lines are calculated $S(Q, \omega)$ curves using eqs 18–22 with $\Gamma_\infty = 0.635 \text{ meV}$, $\sigma_E = 1.1 \text{ kJ mol}^{-1}$, and $E_a = 4.5 \text{ kJ mol}^{-1}$ and fixed EISF values. The only adjustable parameters are $F(Q)$ and $B(Q)$.

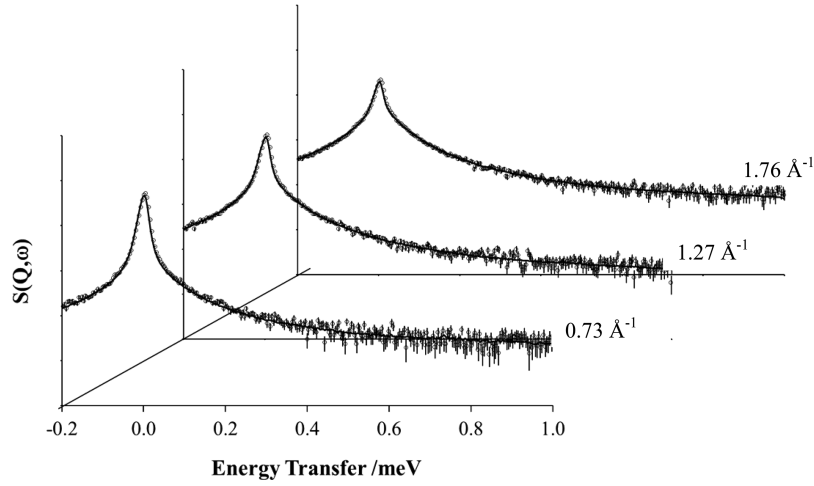


Figure 2. QENS spectra of cyclic PDMS (C445) at 240 K and $Q = 0.73, 1.27, \text{ and } 1.76 \text{ \AA}^{-1}$ (from front to back). Symbols represent experimental data, and lines are calculated $S(Q, \omega)$ curves using eqs 18–22 with $\Gamma_\infty = 0.635 \text{ meV}$, $\sigma_E = 1.1 \text{ kJ mol}^{-1}$, and $E_a = 4.5 \text{ kJ mol}^{-1}$ and fixed EISF values. The only adjustable parameters are $F(Q)$ and $B(Q)$ (eq 22).

dynamics are slower than the temporal range probed by the IRIS and OSIRIS instruments and thus do not contribute to quasi-elastic broadening.^{57,58,61} Bearing this in mind, the incoherent dynamic structure factor can be expressed in terms of the rotational scattering law of the side groups:

$$S_{\text{inc}}(Q, \omega) = \text{DWF}[A_0(Q)\delta(\omega) + S_{\text{inc}}^{\text{qel}}(Q, \omega)] \quad (17)$$

where DWF is the Debye–Waller factor⁷⁵ and $A_0(Q)$ is the elastic incoherent structure factor (EISF), which represents the space-Fourier transform of the final distribution of the scattering centers, averaged over all possible initial positions. For a 3-fold jump rotation, $A_0(Q)$ is given by

$$A_0(Q) = \frac{1}{3}(1 + 2j_0(\sqrt{3}Q \cdot r)) \quad (18)$$

$j_0(x)$ being a zero-order spherical Bessel function and r the distance between the moving protons and the rotation axis. Within the rotational rate distribution model, RRRDM, the quasi-elastic component is described by a log-Gaussian distribution of Lorentzian lines $L_i(\omega)$:^{76,77}

$$S_{\text{inc}}^{\text{qel}}(Q, \omega) = [1 - A_0(Q)] \sum g_i L_i(\omega) \quad (19)$$

where $L_i(\omega) = \frac{1}{\pi} \frac{\Gamma_i}{\Gamma_i^2 + \omega^2}$. The parameter g_i represents the weight of each Lorentzian line:

$$g(\ln \Gamma_i) = \frac{1}{(2\pi\sigma_\Gamma^2)^{0.5}} \exp\left[-\frac{(\ln \Gamma_i - \ln \Gamma_0)^2}{2\sigma_\Gamma^2}\right] \quad (20)$$

with σ_Γ being the width of the distribution of rotational frequencies and Γ_0 the most probable width of the quasi-elastic component. For side group motion, the temperature dependence of the quasi-elastic component is described by the Arrhenius equation:

$$\Gamma_0(T) = \Gamma_\infty \exp\left[-\frac{E_a}{RT}\right] \quad (21)$$

where E_a is the activation energy barrier for rotation, R the gas constant, and Γ_∞ the attempt to escape frequency or jumping frequency at infinite temperature.

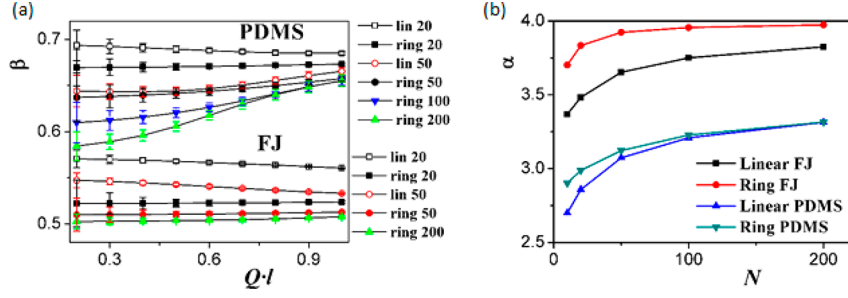


Figure 3. (a) The β exponent plotted vs $Q \cdot l$ for the FJ chain model and for the PDMS chain model with the topology and the selected N values shown in the legend. (b) The α exponent plotted as a function of N for the FJ chain model and for the PDMS chain model with the topology shown in the legend. In both panels, the error bars obtained in the fitting procedure are shown, although in most cases they are smaller than the symbol size.

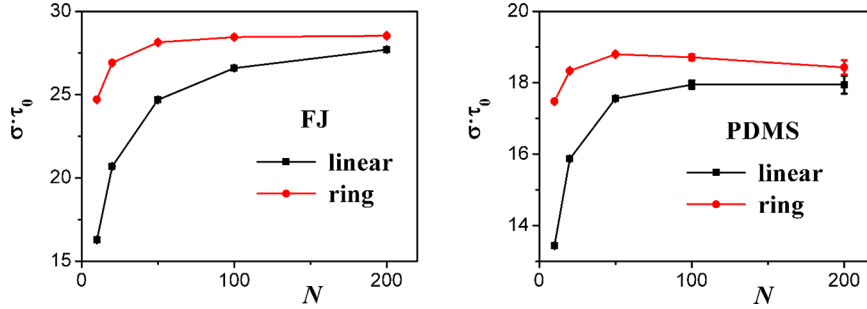


Figure 4. Effective characteristic time τ_0 in σ^{-1} units (see eq 11) plotted as a function of N for (a) the FJ chain model and (b) the PDMS chain model. In both panels, the error bars obtained in the fitting procedure are shown, even though they are smaller than the symbol size.

The above equations are used to fit the experimental data, after convolution with the instrumental resolution, $R(Q, \omega)$, and addition of a flat background, $B(Q)$:

$$S(Q, \omega) = F(Q) \left[A_0(Q) \delta(\omega) + \left((1 - A_0(Q)) \sum_{i=1}^N g_i L_i(\omega) \right) \right] \otimes R(Q, \omega) + B(Q) \quad (22)$$

where the term $F(Q)$ is a temperature and Q dependent scaling factor. The flat background $B(Q)$ represents any fast process outside time window of instrument.

For the purpose of this study, we note that the low-temperature data of cyclic PDMS (C2755) are well represented by eq 22, using parameters reported by us for linear PDMS^{57,58} ($\Gamma_\infty = 0.63 \pm 0.06$ meV, $E_a = 4.5 \pm 0.5$ kJ mol⁻¹, and the width of the distribution of activation energies, $\sigma_E = 1.1 \pm 0.1$ kJ mol⁻¹) and fixed EISF values for the 3-fold methyl group dynamics. The agreement between calculated and experimental values is shown in Figure 1 for $Q = 1.31 \text{ \AA}^{-1}$ at 158, 183, and 208 K.

Perhaps more surprisingly, good agreement between calculated $S(Q, \omega)$ values and experimental data is also found for very small cyclics. As shown in Figure 2 for C445 for $T = 240$ K, calculations closely match the Q dependence of the quasi-elastic broadening. However, deviations are observed at the lowest and highest Q values. Fits using eqs 18–22 are shown in the Supporting Information. We note that the fitting parameters and the corresponding values of Γ_∞ , σ_E , and E_a (see the Supporting Information) are sufficiently close to those reported by us previously,⁵⁷ and so these will be used again here to fit the high-temperature data.

3.2. Theoretical Results. As previously pointed out and also noted in ref 55 for linear chains, the fit of the calculated $I_{\text{inc}}(Q, t)$ using the KWW function was in all cases excellent. The fitted β exponents are reported in Figure 3a as a function of $Q \cdot l$ for the various cases. As a general trend, we find that (i) β increases with the local stiffness of the chain, (ii) β decreases somewhat with an increasing molar mass in particular at small Q values, and (iii) while β is slightly larger for the linear chain than for the ring at very small molar mass, this difference becomes quickly negligible with an increasing molecular length, tending to a value close to about 0.65 as found in ref 55 for linear chains only.

As already done in ref 55, the characteristic time τ depends on Q through the power law

$$\tau = \tau_0 Q^{-\alpha} \quad (23)$$

Also in this case, eq 23 describes very accurately the Q dependence of τ , as shown by the correlation coefficient larger than 0.9990 for the FJ chain and 0.9986 for the PDMS chain model obtained by the fit of τ vs Q .

The fitted values of α plotted as a function of N are shown in Figure 3b. The α exponent is larger for the FJ chain than for the more realistic PDMS chain model having a local stiffness, and it is larger for the ring than for the linear chain. While this difference is very small for the PDMS chain model, unlike for the FJ chain, in both cases α increases monotonically with N , hence with molar mass, to an asymptotic constant value very close to 4 for the latter and most likely independent of the molecular topology. On the other hand, the asymptotic value for the PDMS chain model is smaller, tending to a value close to 3.4 as obtained for much larger linear chains in ref 55.

The τ_0 values obtained from eq 23 are plotted as a function of N in Figure 4. The characteristic time shows an interesting difference between the linear chains and the rings at relatively small molar mass, whereas the asymptotic value for very large N

is independent of molecular topology, as could be expected. In particular, the ring shows a larger τ_0 both in the FJ and in the PDMS chain models. However, this difference becomes negligible for very large N , hence for very large molar masses, so that asymptotically the same τ_0 is achieved for both topologies. Moreover, the results obtained for the more realistic PDMS chain model, accounting for the (albeit limited) conformational rigidity related to the preferred rotational states around the Si–O, show a further slight increase of τ_0 in small rings with $N \approx 50$ compared to the linear chains, thus producing a shallow maximum in Figure 4b. A discussion of the physical origin of these theoretical results is deferred to the later discussion in comparison with the experimental results.

3.3. Analysis of QENS Data at Constant T . The molecular weight of the chain dynamics shows features that are consistent with the theoretical calculations. As shown in Figure 5 and Table

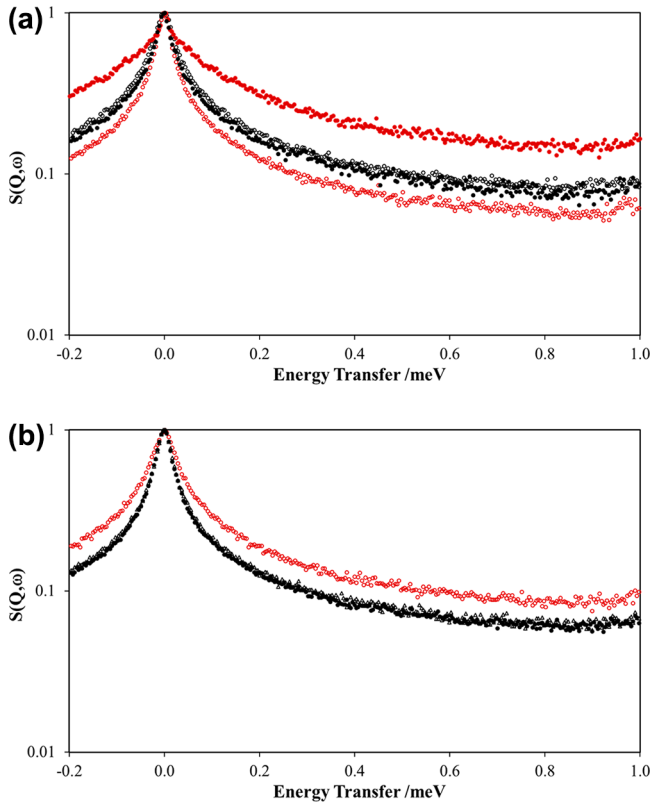


Figure 5. QENS spectra at $Q = 1.45 \text{ \AA}^{-1}$ of (a) L237, L2000, L3800, and L9430 (from top to bottom) and (b) C370 (red \circ), C1200 (\triangle), and C2700 (\bullet) at ca. 110 deg above the sample's T_g . Note: the small upturn for energy transfer values above ca. 0.9 meV is a result of data reduction artifact due to normalization.

1, QENS measurements were performed on a series of linear and cyclic PDMS samples at ≈ 110 deg above the sample's T_g . For all samples, full broadening of the elastic line is observed but changes with molecular weight appear to be more pronounced for the linear than for cyclic PDMS.

A qualitative indication of the dynamic changes due to topology is given in Figure 6 where we compare, at the same temperature (280 K), a cyclic (C1200) and a linear PDMS (L1400) sample with similar average number of monomers ($N_n = 16.4$ and $N_n = 19.3$, respectively).

To extract quantitative information about the molecular weight dependence of the segmental relaxation, we follow our

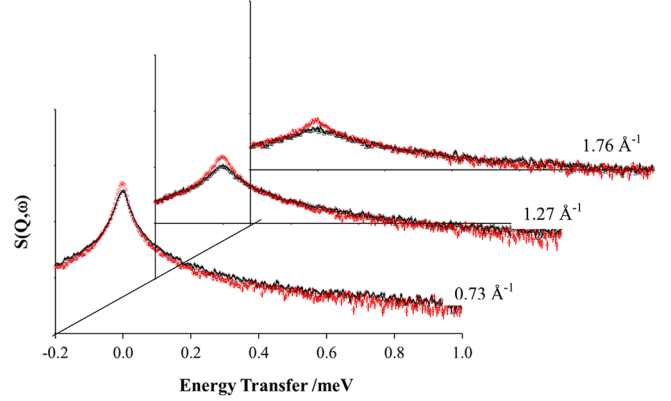


Figure 6. Comparison between QENS spectra of linear and cyclic polymers with similar number of monomers at 280 K and $Q = 0.73$, 1.27, and 1.76 \AA^{-1} : (red \circ) C1200 and (\triangle) L1400. For clarity, error bars are only shown for the cyclic data.

previous QENS analysis of high molecular weight linear PDMS.^{57,58} In that work, we showed that for PDMS CH_3 rotations make a non-negligible contribution to the QE broadening (at least within the time scale of the IRIS spectrometer). Thus, the dynamic incoherent structure factor is described by the convolution of two functions: one representing the local segmental relaxation and the other one the rotational motion of the CH_3 groups.

As discussed in refs 57 and 58, the segmental motion can be expressed by the Fourier transform of the KWW function or equivalent expressions such as the Havriliak–Negami equation.^{78,79} The $S(Q, \omega)$ contribution from methyl group rotations is obtained by extrapolation of data acquired at $T < T_m$ to the desired temperature. This procedure assumes no substantial change, i.e., similar energy landscape,⁸⁰ for the methyl group motion across T_g and T_m . Hence, the model function is given by

$$S(Q, \omega) = F(Q) \left[A_0(Q) \delta(\omega) + \left((1 - A_0(Q)) \times \sum_{i=1}^N g_i L_i(\omega) \right) \right] \otimes S_{\text{KWW}}(Q, \omega) \otimes R(Q, \omega) + B(Q) \quad (24)$$

where $S_{\text{KWW}}(Q, \omega)$ is the Fourier integral of the KWW function (eq 16).

All experimental data collected at temperatures above T_m are well described by eq 24, irrespective of molecular weight and topology. The quality of fits is shown in Figures 7 and 8 for linear (L1400) and cyclic (C2700) PDMS samples of intermediate molecular weights.

At first, the $S(Q, \omega)$ data were fitted at each Q value to determine the Q dependence of the KWW parameters, i.e., the stretched exponent β and the characteristic time τ . As shown in Figure 9, even for very small chains, a unique Q dependence can be identified for Q values above 0.5 \AA^{-1} . In this Q range, β values were found to be Q independent (Figure 10). This finding is consistent with our earlier study of linear high molecular weight PDMS.^{57,58}

To account for differences in the distribution of relaxation times, effective times, τ_{eff} were calculated using the relationship

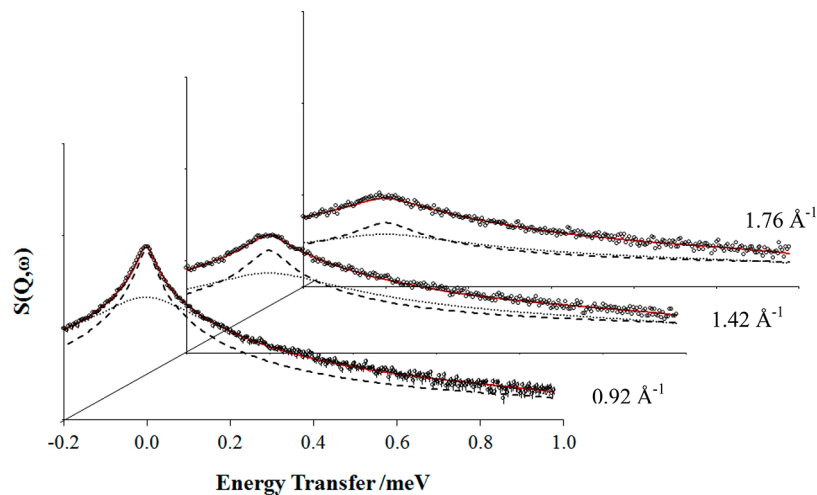


Figure 7. QENS spectra of L1400 at 298 K and Q equal to 0.92, 1.42, and 1.76 \AA^{-1} (from front to back). Symbols represent experimental data while full lines are fits using eq 24. The dashed and dotted lines represent the two dynamic contributions: segmental dynamics (dashed) and methyl rotations (dotted). For clarity, error bars are only shown for one set of data ($Q = 0.92 \text{ \AA}^{-1}$).

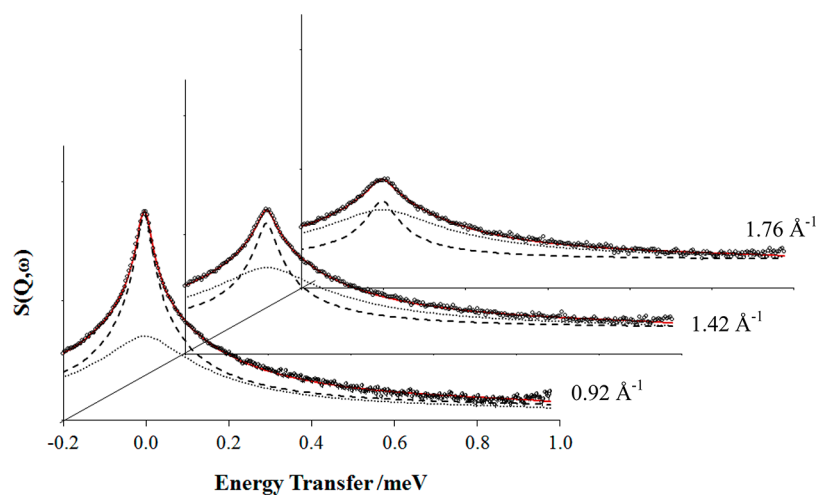


Figure 8. QENS spectra of C2700 at 283 K and Q equal to 0.92, 1.42, and 1.76 \AA^{-1} (from front to back). Symbols represent experimental data while full lines are fits using eq 24. The dashed and dotted lines represent the two dynamic contributions: segmental dynamics (dashed) and methyl rotations (dotted). For clarity, error bars are only shown for one set of data ($Q = 0.92 \text{ \AA}^{-1}$).

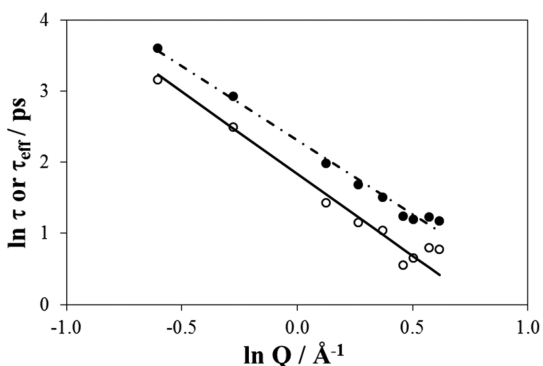


Figure 9. Q dependence of the characteristic time, τ (○) and τ_{eff} (●) (eq 25), as obtained from fitting data of L237 at 235 K using eq 24. The lines represent values obtained by simultaneous fits using eqs 23–25.

$$\tau_{\text{eff}} = \tau \frac{\Gamma\left(\frac{1}{\beta}\right)}{\beta} \quad (25)$$

Values of τ_{eff} are also plotted in Figure 9 and compared to the trend obtained by fitting simultaneously at all Q 's using eqs 23–25.

However, analysis of OSIRIS data for L550 revealed a sharp increase in β values toward unity ($\beta \sim 0.8$) at the lowest Q (Figure 9). This is attributed to contributions from center-of-mass diffusion which, at small Q values, is expected for small molecules. Diffusion of the whole molecule can be described by a single-exponential function corresponding to a Lorentzian line in the frequency domain. In our analysis, this corresponds to a stretched exponent $\beta = 1$.

The OSIRIS data of L550 (Figure 10b) confirm that at $Q > 0.5 \text{ \AA}^{-1}$ β is within experimental error, independent of the momentum transfer, Q .

The molecular weight dependence of the stretched exponent β (Figure 11) seems to suggest a decrease in β values with increasing molar mass for both linear chains and cyclics, reaching a constant value at high M_n which is equal to 0.56 and 0.52 for linear and cyclic polymers, respectively. This seems consistent with the predicted trend (Figure 3) that β increases with decreasing molar mass, and it is lower for cyclics compared

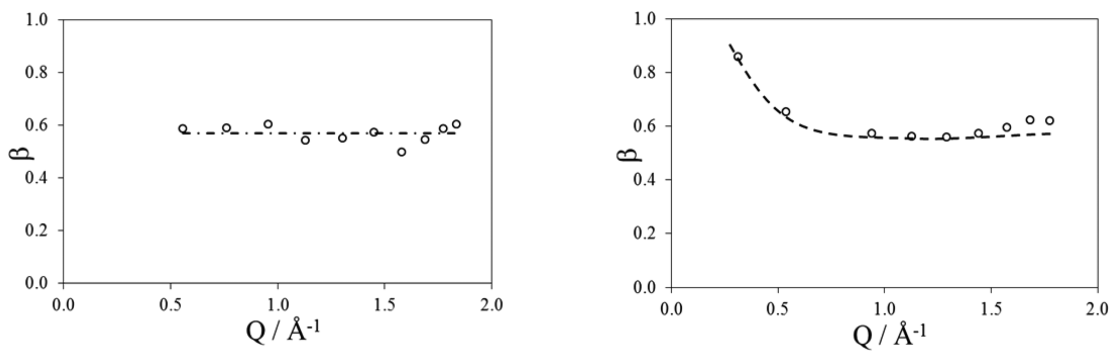


Figure 10. Q dependence of the β parameter as obtained from fitting data of (a) L237 at 235 K (IRIS data) and (b) L550 at 235 K using eq 24. The lines represent a guide to the eye.

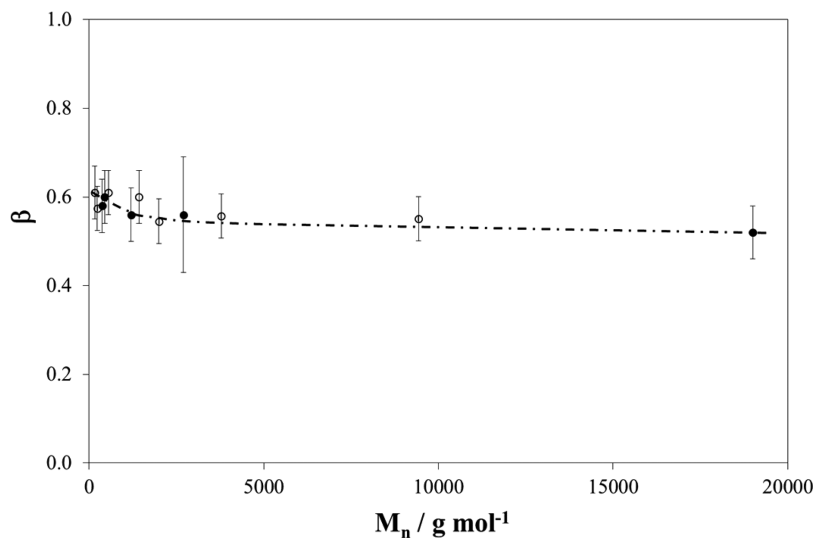


Figure 11. Molar mass dependence of the stretched exponent as obtained from fits of the $S(Q,\omega)$ data at ca. 110 deg above T_g for (○) linear PDMS and (●) cyclic siloxanes. The line is a guide to the eye.

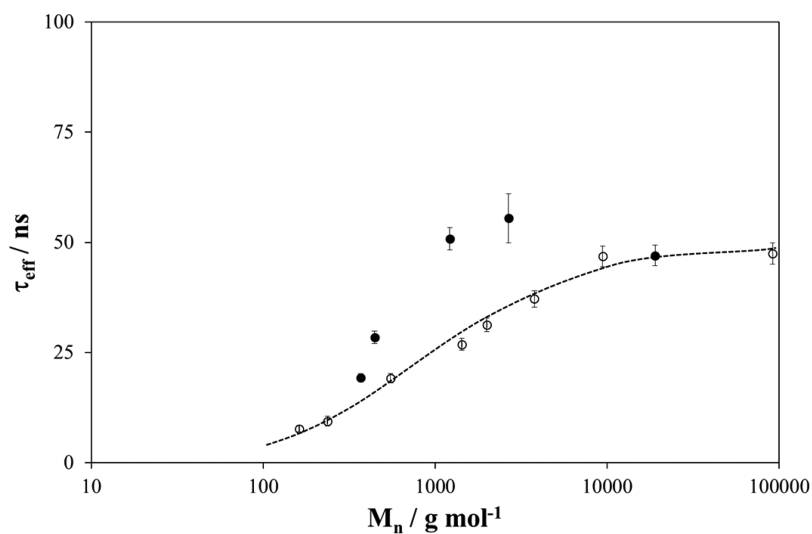


Figure 12. Molar mass dependence of τ_{eff} for linear (○) and cyclic (●) PDMS at ca. 110 deg above the corresponding glass transition. The dotted line is a guide to the eye. Error bars are shown for all data.

to linear chains of the same molecular weight. However, experimental errors on the β values are relatively large, and differences between rings and chains are not statistically significant (Figure 11).

Very few studies of local chain dynamics have been published, and the results are somewhat contradictory. For example, dielectric spectroscopy (DS) measurements performed by Krist et al. found $\beta = 0.485$ for both linear and cyclic polymers,

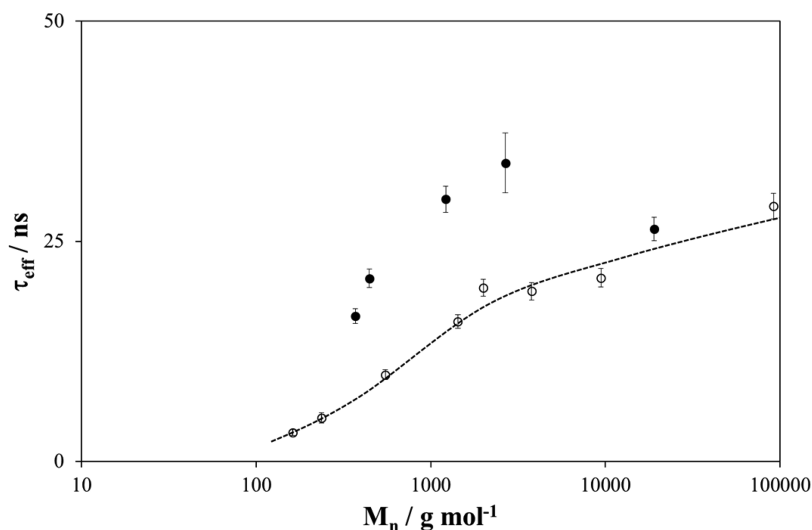


Figure 13. Molar mass dependence of τ_{eff} for linear (O) and cyclic (●) PDMS at 280 K. The dotted line is a guide to the eye. Error bars are shown for all data.

suggesting no change in the distribution of relaxation times with topology.⁶² Similar work by Goodwin et al. reported a slightly lower β average value ($\beta = 0.48$) for linear compared to cyclic ($\beta = 0.53$) PDMS.⁶⁵ This result was taken as an indication that relaxation is more cooperative in linear PDMS.

Here we note that although average β values are lower for cyclics, changes are within experimental error (Figure 11).

To be able to make quantitative comparison between the time scales of the segmental relaxation in PDMS samples, we calculated effective times, τ_{eff} , from τ at $Q = 1 \text{ \AA}^{-1}$, i.e., τ_0 , using eq 25. τ_{eff} values are plotted in Figures 12 and 13 as a function of molecular weight for both linear and cyclic PDMS.

As shown in Figure 12, differences in the glass transition temperature of the samples are not sufficient to account for the molar mass dependence of the relaxation times. For linear siloxanes, τ_{eff} increases, i.e., molecular motion slows down, with increasing molar mass. A similar trend has been reported for polyisobutylene (PIB) by Frick et al.⁸¹ These authors noted that T_g differences and contributions from center-of-mass diffusions at low molar mass could not fully account for the observed dynamic changes with chain length. It was suggested that the discrepancy was due to faster motion of near chain-end groups. This idea was supported by experiments in the glassy state.

Values of τ_{eff} plotted in Figure 12 refer to either measurements performed at $T_g + 110 \text{ }^\circ\text{C}$ or values scaled to this temperature using experimentally determined activation energies (see the following section). The τ_{eff} value reported by us previously for a linear PDMS sample with $M_w = 91700 \text{ g mol}^{-1}$ ($= 47.5 \text{ ps}$), also shown in Figure 12, compares well with the value for the highest

M_n sample investigated here.

The QENS data reported here were collected at Q values above 0.5 \AA^{-1} , and as discussed earlier, little or no contribution from center-of-mass diffusion is expected even for small chains. Therefore, having accounted for T_g changes, the observed trend supports the idea that mobile chain ends are responsible, at low M_n , for the faster dynamics.

The closed structure of rings implies no contribution from fast chain ends. Therefore, one might expect that once T_g changes are accounted for, relaxation times are independent of molar mass. This is not the case for our data (Figure 12), and although τ_{eff} values for cyclic PDMS are higher compared to those of

linear samples, there is a clear M_n dependence. In particular, τ_{eff} increases with increasing degree of polymerization, passes through a maximum value, and for $M_n = 19000 \text{ g mol}^{-1}$ approaches values characteristic of linear chains. On the other hand, this trend is consistent with theoretical predictions in terms of τ_0 (eq 23 and Figure 4). To understand this behavior, it should be noted that the local segmental relaxation proceeds through the conformational rearrangements around the chemical bonds of the main chain. Thus, the ring shows a lengthier relaxation due to the topological constraint imposed by the ring closure: this feature slows down the local dynamics compared to the linear chain whose dynamics is faster thanks to its free ends. This effect is already evident in the FJ chain model devoid of any local rigidity and corresponding to the familiar bead-and-spring chain. Moreover, it is further enhanced in the PDMS chain model by the additional constraint of the (limited) conformational rigidity related to the preferred rotational states around the Si–O bonds, as anticipated, producing a shallow maximum (Figure 4b). Qualitatively, a similar trend is displayed by our experimental results (Figure 12).

Figure 12 suggests that the dynamics of small rings is not that different from motion of very short chains. However, one should bear in mind that τ_{eff} values reported in Figure 12 were obtained in some cases at considerably different temperatures. For example, there is a 40° difference between τ_{eff} of C370, measured at 275 K, and the corresponding value for L237, measured at 235

K. To appreciate how τ_{eff} changes with molar mass and topology, we have reported in Figure 13 values at a common temperature of 280 K. Greater changes with topology can be observed in this case since differences in T_g are not accounted for.

Finally, we note that the exponent, α , obtained by assuming a power law dependence of the characteristic time (eq 23) was found to vary in the range 1.86 ± 0.05 for L162 to 2.5 ± 0.1 for L1400. These values are lower than those obtained by us for linear high molecular weight PDMS (α ca. 2.3),^{55,57,58} suggesting a very weak, if any, molecular weight dependence. We note that larger values are obtained if methyl group rotations are not accounted for with α in the range 3.0–3.3 for high molecular weight PDMS, depending on temperature. It is also interesting to point out that the values of α in the latter range nicely agree with the theoretical ones reported for the PDMS

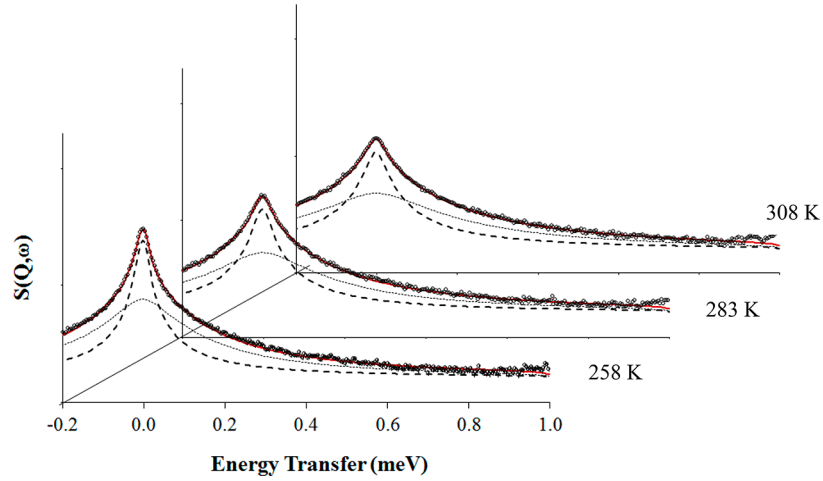


Figure 14. QENS spectra of C2755 at $Q = 1.45 \text{ \AA}^{-1}$ and three temperatures above T_g : 258, 283, and 308 K (from front to back). Symbols represent experimental data while full lines are fits using eq 24. The dashed and dotted lines represent the two dynamic contributions: segmental dynamics (dashed) and methyl rotations (dotted).

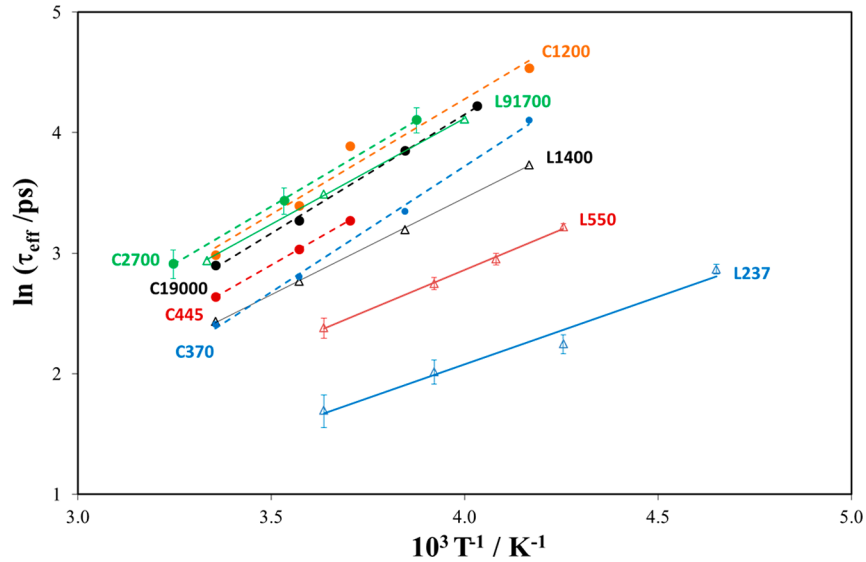


Figure 15. Temperature dependence of τ_{eff} for linear and cyclic PDMS samples. The lines are fits to the experimental points using the Arrhenius equation. Error bars are shown for selected data: L237, L550, and C2700.

chain model in Figure 3b where the methyl group rotation is also ignored. Similar observations were made by Frick et al.,⁸¹ who studied the molecular weight and Q dependence of the relaxation times of PIB at 368 K from 0.2 to 1.9 \AA^{-1} . In that work, a change from $\tau \propto Q^{-2/\beta}$ at low Q to $\tau \propto Q^{-2}$ at high Q was observed for samples with M_w ranging from 680 to 73000 g mol^{-1} . Our data samples relatively high Q values, and such crossover is not evident.

For cyclic PDMS similar α values were obtained within a relatively narrow range from 2.1 to 2.8, depending on molar mass and temperature (the error in all cases is estimated to be ca. 0.2).

3.4. Temperature Dependence of Segmental Motion for Linear and Cyclic PDMS. As briefly mentioned in the previous section, in addition to measurements performed at equal distance from T_g , QENS data were also collected for selected linear and cyclic samples at a series of temperatures above T_m . To simplify data analysis, the $S(Q, \omega)$ spectra were fitted simultaneously using a constant β and $\tau = \tau_0 Q^{-\alpha}$. Example

of fits are shown in Figure 14 for C2755 at $T = 258, 283,$ and 308 K.

The temperature and molar mass dependence of τ_{eff} for all samples investigated is shown in Figure 15. As shown by us elsewhere for PDMS samples at T above T_m , both viscosity and relaxation times follow an Arrhenius temperature dependence:^{55,57,58}

$$\tau_{\text{eff}} = \tau_{\infty} e^{E_a/RT} \quad (26)$$

where E_a is the activation energy, R the gas constant, and τ_{∞} is the relaxation time at infinite temperature.

As shown in Figure 15, eq 26 applies to all QENS data, irrespective of molar mass and topology. The variations in τ_{eff} values mimic the trend reported earlier (Figures 12 and 13). For linear chains relaxation times are strongly dependent upon molar mass, increasing as M_n increases. However, for cyclic PDMS, τ_{eff} increases from C370 to C2700 and consistently lower values are obtained for C19000, at all temperatures (even below those of the linear samples).

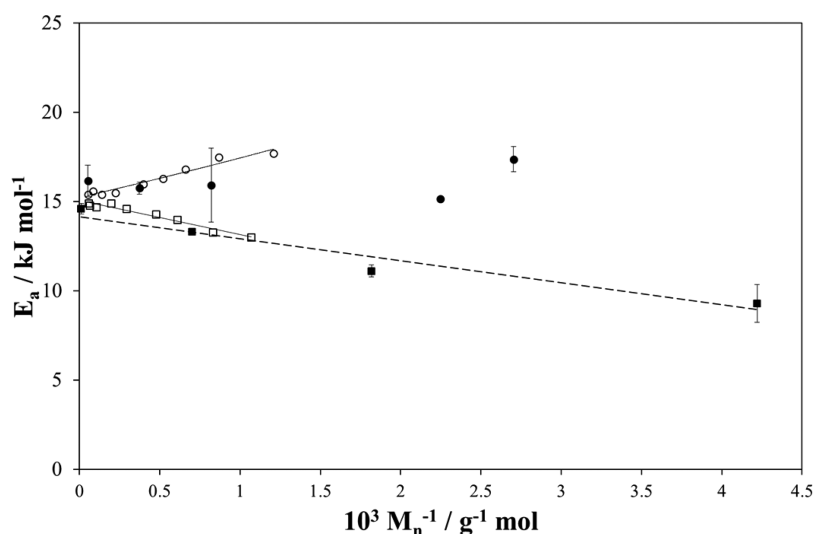


Figure 16. Molar mass dependence of the activation energy for segmental motion as determined from data in Figure 15 using eq 26: linear PDMS (solid squares) and cyclic PDMS (solid circles). Experimental data are compared with activation energies of linear (open squares) and cyclic (open circles) PDMS from the rheological measurements reported in ref 10. Lines are guides to the eye.

Activation energies can be calculated from the slope of $\ln \tau_{\text{eff}}$ versus $1/T$ (Figure 15). E_a values are plotted in Figure 16 for both cyclic and linear PDMS and compared to literature data from bulk viscosity measurements of Dodgson et al.^{10–12}

At first inspection, agreement with viscosity measurements appears to be closer for linear than for cyclic PDMS. For linear chains, E_a increases with increasing molar mass from 9.3 ± 1.0 kJ mol^{-1} for L237 to 14.6 ± 0.3 kJ mol^{-1} , the value reported by us for L91700 in ref 49.

Viscosity data of Dodgson et al.^{10–12} show that for cyclic PDMS activation energies decrease with increasing molar mass, contrary to the increase of E_a values observed for linear PDMS with increasing M_n . For both cyclic and linear PDMS a constant value is reached at high molar mass which is equal to ~ 14.8 kJ mol^{-1} for the linear samples. For cyclics, a higher value (~ 15.5 kJ mol^{-1}) was obtained.

Although our data provide clear evidence that activation energies are higher for cyclics compared to linear chains, there is no unambiguous trend with molar mass. Values range from 17.4 ± 0.7 kJ mol^{-1} for C370 to 16.2 ± 0.9 kJ mol^{-1} for C19000. The relatively high value recorded for C370 is not unexpected based on QENS measurements of small rings carried out several years ago by us where a value of 21 kJ mol^{-1} was reported for hexamethylcyclotrisiloxane ($M_n = 222.5$ g mol^{-1}). However, the reason why there is such a discrepancy between E_a values of C370 and C445 (15.2 ± 0.1 kJ mol^{-1}) is at present unclear.

4. CONCLUSION

A detailed investigation of local dynamics of linear and cyclic PDMS as a function of molar mass has been presented. QENS experiments in the time scale from 2 to 200 ps and at $Q = 0.3$ to 1.8 \AA^{-1} were complemented by theoretical calculations performed (a) within the framework of a freely jointed (FJ) chain model devoid of any local correlation among the rotational states and equivalent to a fully flexible bead-and-spring chain and (b) for a realistic PDMS chain within the rotational isomeric state approach considering the monomeric $-\text{Si}(\text{CH}_3)_2-\text{O}-$ as the repeat unit.

At low temperature, the experimental results show that the rotational motion of the methyl groups provides the main

contribution to the quasi-elastic broadening. The $S(Q, \omega)$ data of cyclic PDMS can be represented by the same model used for linear chains.^{57,58} Our findings show that the methyl group rotation is described by the same parameters reported for a linear PDMS sample with $M_w = 91700$ g mol^{-1} , irrespective of molar mass and topology.

To extract information about segmental motion, a series of QENS measurements were performed at temperatures above T_m , i.e., in the melt state. Using the same procedure established for high molecular weight PDMS, we used a model function that explicitly accounts for contributions from methyl group rotation and segmental motion.^{57,58} For the segmental relaxation, measurements performed at a constant distance from T_g show that the stretching exponent slightly decreases from $\beta \sim 0.6$ at low molar mass to values approaching 0.56 for linear chains. No clear evidence for differences between β values of linear and cyclic chains was found, within experimental error. We note that β values higher than 0.5 are predicted by theory and attributed to chain stiffness effects that increase with decreasing chain length.

Several features predicted by theory are also reproduced by the experimental data. Specifically, relaxation times of both linear and cyclic PDMS at temperatures equally distant from their T_g s increase with increasing molecular weight. Perhaps more importantly, rings display higher relaxation times for the local segmental motion, i.e., relax at a slower rate, compared to linear chains of the same molar mass. This is true even when differences among glass transition temperatures are accounted for.

Theoretical calculations support the idea that the topological constraint imposed by the ring closure slows down the local dynamics compared to a linear chain. For very large molar masses, this constraint becomes negligible and so the same τ_{eff} is achieved for both topologies. Interestingly, it is suggested by our calculations that due to its conformational rigidity, PDMS undergoes an additional constraint which further increases τ_{eff} , thus producing a shallow maximum for $N \approx 50$ (Figure 4b).

Evidence for a broad maximum in τ_{eff} is also observed in the experimental QENS data (Figures 12 and 13).

Furthermore, the activation energy of cyclic PDMS is higher than that of linear chains, values being in reasonable agreement

with viscosity measurements.^{10–12} The pronounced molecular weight dependence of E_a for linear PDMS is primarily linked to the presence of mobile chain ends.

In light of recent work on the dynamics of cyclic and linear chains,^{38,50,82} our finding that cyclic PDMS is slower compared to linear PDMS chains may seem at first surprising. This is due to the very low molecular weight samples studied in this work and the fact that using QENS, we are probing dynamics on a short length scale of the order of a few statistical units. We would also like to stress that the anomalous behavior observed for cyclic PDMS occurs within a molecular weight region that is unaffected by contamination from linear chains.

The cyclic PDMS fractions investigated in this work were prepared by ring–ring equilibration process.⁸³ As noted by Kricheldorf, equilibrations of polysiloxanes and cyclosiloxanes have been studied by several research groups.¹ At high dilution, data show that “equilibration of cyclic monomers or oligomers allows for preparation of polydisperse cyclic polymers almost free from linear chains”.¹ Ring–ring equilibration is an equilibrium process, and so calculation of the ring and chain fractions for each M_w is possible. Using data reported by Semlyen, we estimate that there is $\approx 8\%$ contamination by linear chains in samples with $M_w = 17000 \text{ g mol}^{-1}$. This reduces to 1% for $M_w = 8400 \text{ g mol}^{-1}$, and it is vanishingly small for $M_w = 3990 \text{ g mol}^{-1}$.⁸³

As shown by the τ_{eff} versus M_w data (Figure 12), local chain dynamics is unaffected by the presence of entanglements: τ_{eff} approaching constant values at higher M_w . As expected, τ_{eff} values mimic the T_g dependence upon M_w rather than the molecular weight dependence of the viscosity or long time dynamics. It is therefore reasonable to expect that within the time and distance scale of our experiments the dynamics of large cyclics cannot be distinguished from that of linear chains (Figure 12). In this regime, contamination by a small amount of linear chains has no effect on the outcome. Obviously, linear chain contamination of cyclic fractions crucially affects terminal relaxation behavior⁸⁴ and long chain dynamics as observed in NSE experiments above the entanglement molecular weight.

Our experiments and calculations based on siloxanes show changes with topology that are not only in agreement with previous QENS data⁵⁶ but also support findings from bulk viscosity measurements^{10–12} as well as self-diffusion and spin–spin relaxation measurements¹⁵ according to which rings have slower dynamics (higher viscosities or smaller diffusion coefficients) compared to linear chains at low molar mass. As noted earlier, the viscosity data of Semlyen et al. exhibit opposite behavior in the high molar mass range, above the entanglement molecular weight, M_e . Such a crossover from slower to faster dynamics has been reported by Ozisik et al.⁸⁵ and Hur et al.^{25,26} in their computer simulations of cyclic and linear polyethylenes. We note that experimental studies of ring dynamics have often been performed on high molar mass samples, above M_e ,^{38,50,82} and therefore no direct comparison can be made with our experimental data. However, for poly(oxyethylene)s, Nam et al.⁵² measured self-diffusion, NMR spin–spin relaxation, and zero shear rate viscosities of monodisperse, low molecular weight cyclic ($400\text{--}1500 \text{ g mol}^{-1}$) and linear samples, reporting slower dynamics for poly(oxyethylene) rings.

As discussed in previous sections, the faster motion of linear chains cannot be simply attributed to chain end effects; dynamic differences are still evident even after scaling at constant segmental mobility. Other effects such as frustration of segmental rotational diffusion in small rings and the configura-

tional entropy of rings, which is generally much smaller than that of the linear chains,⁶² also need to be considered. As noted earlier, molecular motion observed by QENS is due to conformational rearrangements along the polymer backbone. This, being essentially an intramolecular process, is affected by the closure constraint in cyclic molecules which slows down the segmental relaxation. The smaller the ring, the more pronounced is this effect. It remains to be seen whether this is a feature of the PDMS samples investigated here or it is applicable to other cyclic systems such as cyclic PEO or alkanes.

ASSOCIATED CONTENT

Supporting Information

The Supporting Information is available free of charge on the ACS Publications website at DOI: 10.1021/acs.macromol.8b00397.

Figure A1 showing low-temperature QENS data of a cyclic PDMS sample and fits (PDF)

AUTHOR INFORMATION

Corresponding Author

*(V.A.) Fax +44 (0) 131 451 3180; phone +44 (0) 131 451 3108, e-mail v.arrighi@hw.ac.uk.

ORCID

Valeria Arrighi: 0000-0002-4245-3249

Fabio Ganazzoli: 0000-0002-9762-4535

Present Address

J.T.: Esso (Thailand), Thoongsukla, Sriracha, Chonburi 20230, Thailand.

Notes

The authors declare no competing financial interest.

ACKNOWLEDGMENTS

We thank the ISIS (Rutherford Appleton Laboratory, UK) for beam time and Prof. P. Griffiths for kindly giving us some of the cyclic samples. We acknowledge the important work carried out over many years by the late Dr. J. A. Semlyen on cyclic polymers. Without his contribution, and that of his co-workers, this work would have not been possible.

REFERENCES

- (1) Kricheldorf, H. R. Cyclic Polymers: Synthetic Strategies and Physical Properties. *J. Polym. Sci., Part A: Polym. Chem.* **2010**, *48* (2), 251–284.
- (2) Ungar, G.; Zeng, K. B. Learning polymer crystallization with the aid of linear, branched and cyclic model compounds. *Chem. Rev.* **2001**, *101* (12), 4157–4188.
- (3) Su, H.-H.; Chen, H.-L.; Diaz, A.; Teresa Casas, M.; Puiggali, J.; Hoskins, J. N.; Grayson, S. M.; Perez, R. A.; Mueller, A. J. New insights on the crystallization and melting of cyclic PCL chains on the basis of a modified Thomson-Gibbs equation. *Polymer* **2013**, *54* (2), 846–859.
- (4) Clarson, S. J.; Dodgson, K.; Semlyen, J. A. Studies of Cyclic and Linear Poly(dimethylsiloxane). 19. Glass-transition Temperatures and Crystallization Behavior. *Polymer* **1985**, *26* (6), 930–934.
- (5) Huang, D. H.; Simon, S. L.; McKenna, G. B. Chain length dependence of the thermodynamic properties of linear and cyclic alkanes and polymers. *J. Chem. Phys.* **2005**, *122* (8), 084907.
- (6) Dimarzio, E. A.; Guttman, C. M. The Glass Temperature of Polymer Rings. *Macromolecules* **1987**, *20* (6), 1403–1407.
- (7) Liu, X. J.; Chen, D. L.; He, Z. D.; Zhang, H.; Hu, H. Z. Molecular-weight Dependence of the Glass-transition of Cyclic Polystyrene. *Polym. Commun.* **1991**, *32* (4), 123–125.

- (8) Gan, Y. D.; Dong, D. H.; Hogenesch, T. E. Effects of lithium bromide on the glass-transition temperatures of linear and macrocyclic poly(2-vinylpyridine) and polystyrene. *Macromolecules* **1995**, *28* (1), 383–385.
- (9) Santangelo, P. G.; Roland, C. M.; Chang, T.; Cho, D.; Roovers, J. Dynamics near the glass temperature of low molecular weight cyclic polystyrene. *Macromolecules* **2001**, *34* (26), 9002–9005.
- (10) Dodgson, K.; Bannister, D. J.; Semlyen, J. A. Studies of Cyclic and Linear Poly(dimethyl siloxanes). 4. Bulk Viscosities. *Polymer* **1980**, *21* (6), 663–667.
- (11) Orrah, D. J.; Semlyen, J. A.; Rossmurphy, S. B. Studies of Cyclic and Linear Poly(Dimethylsiloxanes) 0.27. Bulk Viscosities above the Critical Molar Mass for Entanglement. *Polymer* **1988**, *29* (8), 1452–1454.
- (12) Orrah, D. J.; Semlyen, J. A.; Rossmurphy, S. B. Studies of Cyclic and Linear Poly(Dimethylsiloxanes) 0.28. Viscosities and Densities of Ring and Chain Poly(Dimethylsiloxane) Blends. *Polymer* **1988**, *29* (8), 1455–1458.
- (13) Mills, P. J.; Mayer, J. W.; Kramer, E. J.; Hadziioannou, G.; Lutz, P.; Strazielle, C.; Rempp, P.; Kovacs, A. J. Diffusion of Polymer Rings in Linear Polymer Matrices. *Macromolecules* **1987**, *20* (3), 513–518.
- (14) Tead, S. F.; Kramer, E. J.; Hadziioannou, G.; Antonietti, M.; Sillescu, H.; Lutz, P.; Strazielle, C. Polymer Topology and Diffusion - A Comparison of Diffusion In Linear and Cyclic Macromolecules. *Macromolecules* **1992**, *25* (15), 3942–3947.
- (15) Cosgrove, T.; Griffiths, P. C.; Hollingshurst, J.; Richards, R. D. C.; Semlyen, J. A. Self-Diffusion and Spin Spin Relaxation in Cyclic and Linear Polydimethylsiloxane Melts. *Macromolecules* **1992**, *25* (25), 6761–6764.
- (16) Cosgrove, T.; Turner, M. J.; Griffiths, P. C.; Hollingshurst, J.; Shenton, M. J.; Semlyen, J. A. Self-diffusion and spin-spin relaxation in blends of linear and cyclic polydimethylsiloxane melts. *Polymer* **1996**, *37* (9), 1535–1540.
- (17) Zimm, B. H.; Stockmayer, W. H. The dimensions of chain molecules containing branches and rings. *J. Chem. Phys.* **1949**, *17*, 1301.
- (18) Casassa, E. F. Some statistical properties of flexible ring polymers. *J. Polym. Sci., Part A: Gen. Pap.* **1965**, *3*, 605.
- (19) Burchard, W.; Schmidt, M. Static and Dynamic Structure Factors Calculated For Flexible Ring Macromolecules. *Polymer* **1980**, *21* (7), 745–749.
- (20) Cates, M. E.; Deutsch, J. M. Conjectures on the Statistics of Ring Polymers. *J. Phys.* **1986**, *47* (12), 2121–2128.
- (21) Klein, J. Dynamics of Entangled Linear, Branched, and Cyclic Polymers. *Macromolecules* **1986**, *19* (1), 105–118.
- (22) Brown, S.; Szamel, G. Computer simulation study of the structure and dynamics of ring polymers. *J. Chem. Phys.* **1998**, *109* (14), 6184–6192.
- (23) Brown, S.; Szamel, G. Structure and dynamics of ring polymers. *J. Chem. Phys.* **1998**, *108* (12), 4705–4708.
- (24) Deutsch, J. M. Equilibrium size of large ring molecules. *Phys. Rev. E: Stat. Phys., Plasmas, Fluids, Relat. Interdiscip. Top.* **1999**, *59* (3), R2539–R2541.
- (25) Hur, K.; Jeong, C.; Winkler, R. G.; Lacevic, N.; Gee, R. H.; Yoon, D. Y. Chain Dynamics of Ring and Linear Polyethylene Melts from Molecular Dynamics Simulations. *Macromolecules* **2011**, *44* (7), 2311–2315.
- (26) Hur, K.; Winkler, R. G.; Yoon, D. Y. Comparison of ring and linear polyethylene from molecular dynamics simulations. *Macromolecules* **2006**, *39* (12), 3975–3977.
- (27) Suzuki, J.; Takano, A.; Matsushita, Y. Topological effect in ring polymers investigated with Monte Carlo simulation. *J. Chem. Phys.* **2008**, *129* (3), 034903.
- (28) Suzuki, J.; Takano, A.; Deguchi, T.; Matsushita, Y. Dimension of ring polymers in bulk studied by Monte-Carlo simulation and self-consistent theory. *J. Chem. Phys.* **2009**, *131* (14), 144902.
- (29) Muller, M.; Wittmer, J. P.; Cates, M. E. Topological effects in ring polymers: A computer simulation study. *Phys. Rev. E: Stat. Phys., Plasmas, Fluids, Relat. Interdiscip. Top.* **1996**, *53* (5), 5063–5074.
- (30) Higgins, J. S.; Dodgson, K.; Semlyen, J. A. Studies of Cyclic And Linear Poly(dimethyl siloxanes) 0.3. Neutron-Scattering Measurements of the Dimensions of Ring and Chain Polymers. *Polymer* **1979**, *20* (5), 553–558.
- (31) Edwards, C. J. C.; Richards, R. W.; Stepto, R. F. T.; Dodgson, K.; Higgins, J. S.; Semlyen, J. A. Studies of Cyclic And Linear Poly(dimethyl siloxanes). 14. Particle Scattering Functions. *Polymer* **1984**, *25* (3), 365–368.
- (32) Roovers, J.; Toporowski, P. M. Synthesis of High Molecular-Weight Ring Polystyrenes. *Macromolecules* **1983**, *16* (6), 843–849.
- (33) Roovers, J. Melt Properties of Ring Polystyrenes. *Macromolecules* **1985**, *18* (6), 1359–1361.
- (34) Takano, A.; Ohta, Y.; Masuoka, K.; Matsubara, K.; Nakano, T.; Hieno, A.; Itakura, M.; Takahashi, K.; Kinugasa, S.; Kawaguchi, D.; Takahashi, Y.; Matsushita, Y. Radii of Gyration of Ring-Shaped Polystyrenes with High Purity in Dilute Solutions. *Macromolecules* **2012**, *45* (1), 369–373.
- (35) Takano, A.; Kushida, Y.; Ohta, Y.; Masuoka, K.; Matsushita, Y. The second virial coefficients of highly-purified ring polystyrenes in cyclohexane. *Polymer* **2009**, *50* (5), 1300–1303.
- (36) Arrighi, V.; Gagliardi, S.; Dagger, A. C.; Semlyen, J. A.; Higgins, J. S.; Shenton, M. J. Conformation of cyclic and linear chain polymers in bulk by SANS. *Macromolecules* **2004**, *37* (21), 8057–8065.
- (37) Gagliardi, S.; Arrighi, V.; Ferguson, R.; Dagger, A. C.; Semlyen, J. A.; Higgins, J. S. On the difference in scattering behavior of cyclic and linear polymers in bulk. *J. Chem. Phys.* **2005**, *122* (6), 064904.
- (38) Bras, A. R.; Pasquino, R.; Koukoulas, T.; Tsolou, G.; Holderer, O.; Radulescu, A.; Allgaier, J.; Mavrantzas, V. G.; Pyckhout-Hintzen, W.; Wischniewski, A.; Vlassopoulos, D.; Richter, D. Structure and dynamics of polymer rings by neutron scattering: breakdown of the Rouse model. *Soft Matter* **2011**, *7* (23), 11169–11176.
- (39) Beaucage, G.; Kulkarni, A. S. Dimensional Description of Cyclic Macromolecules. *Macromolecules* **2010**, *43* (1), 532–537.
- (40) de Gennes, P.-G. Reptation of a polymer chain in the presence of fixed obstacles. *J. Chem. Phys.* **1971**, *55*, 572.
- (41) Doi, M.; Edwards, S. Dynamics of concentrated polymer systems. Part 1.—Brownian motion in the equilibrium state. *J. Chem. Soc., Faraday Trans. 2* **1978**, *74*, 1789–1801.
- (42) Doi, M.; Edwards, S. Dynamics of concentrated polymer systems. Part 2.—Molecular motion under flow. *J. Chem. Soc., Faraday Trans. 2* **1978**, *74*, 1802–1817.
- (43) Doi, M.; Edwards, S. Dynamics of concentrated polymer systems. Part 4.—Rheological properties. *J. Chem. Soc., Faraday Trans. 2* **1979**, *75*, 38–54.
- (44) Klein, J.; Fletcher, D.; Fetters, L. J. Diffusional Behavior of Entangled Star Polymers. *Nature* **1983**, *304* (5926), 526–527.
- (45) Hild, G.; Strazielle, C.; Rempp, P. Cyclic Macromolecules - Synthesis and Characterization of Ring-Shaped Polystyrenes. *Eur. Polym. J.* **1983**, *19* (8), 721–727.
- (46) McKenna, G. B.; Plazek, D. J. Measurement of the Viscoelastic Properties of Blends of Linear and Cyclic Macromolecules. *Abstr. Pap. Am. Chem. Soc.* **1987**, *193*, 161–POLY.
- (47) McKenna, G. B.; Hostetter, B. J.; Hadjichristidis, N.; Fetters, L. J.; Plazek, D. J. A Study of the Linear Viscoelastic Properties of Cyclic Polystyrenes Using Creep and Recovery Measurements. *Macromolecules* **1989**, *22* (4), 1834–1852.
- (48) Kapnistos, M.; Lang, M.; Vlassopoulos, D.; Pyckhout-Hintzen, W.; Richter, D.; Cho, D.; Chang, T.; Rubinstein, M. Unexpected power-law stress relaxation of entangled ring polymers. *Nat. Mater.* **2008**, *7* (12), 997–1002.
- (49) Kawaguchi, D.; Masuoka, K.; Takano, A.; Tanaka, K.; Nagamura, T.; Torikai, N.; Dalglish, R. M.; Langridge, S.; Matsushita, Y. Comparison of interdiffusion behavior between cyclic and linear polystyrenes with high molecular weights. *Macromolecules* **2006**, *39* (16), 5180–5182.
- (50) Richter, D.; Goossen, S.; Wischniewski, A. Celebrating Soft Matter's 10th Anniversary: Topology matters: structure and dynamics of ring polymers. *Soft Matter* **2015**, *11* (44), 8535–8549.

- (51) Roovers, J. Viscoelastic Properties of Polybutadiene Rings. *Macromolecules* **1988**, *21* (5), 1517–1521.
- (52) Nam, S.; Leisen, J.; Breedveld, V.; Beckham, H. W. Dynamics of unentangled cyclic and linear poly(oxyethylene) melts. *Polymer* **2008**, *49* (25), 5467–5473.
- (53) Doi, Y.; Matsumoto, A.; Inoue, T.; Iwamoto, T.; Takano, A.; Matsushita, Y.; Takahashi, Y.; Watanabe, H. Re-examination of terminal relaxation behavior of high-molecular-weight ring polystyrene melts. *Rheol. Acta* **2017**, *56* (6), 567–581.
- (54) Pasquino, R.; Vasilakopoulos, T. C.; Jeong, Y. C.; Lee, H.; Rogers, S.; Sakellariou, G.; Allgaier, J.; Takano, A.; Bras, A. R.; Chang, T.; Goossen, S.; Pyckhout-Hintzen, W.; Wischniewski, A.; Hadjichristidis, N.; Richter, D.; Rubinstein, M.; Vlassopoulos, D. Viscosity of Ring Polymer Melts. *ACS Macro Lett.* **2013**, *2* (10), 874–878.
- (55) Ganazzoli, F.; Raffaini, G.; Arrighi, V. The stretched-exponential approximation to the dynamic structure factor in non-entangled polymer melts. *Phys. Chem. Chem. Phys.* **2002**, *4* (15), 3734–3742.
- (56) Allen, G.; Brier, P. N.; Goodyear, G.; Higgins, J. S. Motional broadening of the quasi-elastic peak in neutrons scattered from polymeric materials. *Faraday Symp. Chem. Soc.* **1972**, *6* (0), 169–175.
- (57) Arrighi, V.; Gagliardi, S.; Zhang, C. H.; Ganazzoli, F.; Higgins, J. S.; Ocone, R.; Telling, M. T. F. A unified picture of the local dynamics of poly(dimethylsiloxane) across the melting point. *Macromolecules* **2003**, *36* (23), 8738–8748.
- (58) Arrighi, V.; Ganazzoli, F.; Zhang, C. H.; Gagliardi, S. New interpretation of local dynamics of poly(dimethyl siloxane) observed by quasielastic neutron scattering. *Phys. Rev. Lett.* **2003**, *90* (5), 058301.
- (59) Fetters, L. J.; Lohse, D. J.; Richter, D.; Witten, T. A.; Zirkel, A. Connection between Polymer Molecular-Weight, Density, Chain Dimensions, and Melt Viscoelastic Properties. *Macromolecules* **1994**, *27* (17), 4639–4647.
- (60) Dvornic, P. R.; Jovanovic, J. D.; Govedarica, M. N. On the Critical Molecular Chain-Length of Polydimethylsiloxane. *J. Appl. Polym. Sci.* **1993**, *49* (9), 1497–1507.
- (61) Grapengeter, H. H.; Alefeld, B.; Kosfeld, R. An Investigation of Micro-Brownian Motions in Polydimethylsiloxane by Complementary Incoherent-Neutron-Scattering and Nmr Experiments Below Room-Temperature. *Colloid Polym. Sci.* **1987**, *265* (3), 226–233.
- (62) Kirst, K. U.; Kremer, F.; Pakula, T.; Hollingshurst, J. Molecular-Dynamics of Cyclic and Linear Poly(dimethylsiloxanes). *Colloid Polym. Sci.* **1994**, *272* (11), 1420–1429.
- (63) Roland, C. M.; Nagi, K. L. Segmental relaxation in poly(dimethylsiloxane). *Macromolecules* **1996**, *29* (17), 5747–5750.
- (64) Goodwin, A. A.; Beevers, M. S.; Clarson, S. J.; Semlyen, J. A. Cyclic polysiloxanes 0.6. Dielectric relaxation of polymethylphenylsiloxanes. *Polymer* **1996**, *37* (13), 2597–2602.
- (65) Goodwin, A. A.; Beevers, M. S.; Clarson, S. J.; Semlyen, J. A. Studies of cyclic and linear polydimethylsiloxanes 0.32. Dielectric relaxation investigations. *Polymer* **1996**, *37* (13), 2603–2607.
- (66) Smith, J. S.; Borodin, O.; Smith, G. D. A quantum chemistry based force field for poly(dimethylsiloxane). *J. Phys. Chem. B* **2004**, *108* (52), 20340–20350.
- (67) Allen, G.; Higgins, J. S.; Wright, C. J. Segmental Diffusion in Rubbers Studied by Neutron Quasi-Elastic Incoherent-Scattering. *J. Chem. Soc., Faraday Trans. 2* **1974**, *70*, 348–355.
- (68) Cowie, J.; McEwen, I. Molecular motions in poly (dimethyl siloxane) oligomers and polymers. *Polymer* **1973**, *14* (9), 423–426.
- (69) Agapov, A. L.; Sokolov, A. P. Does the Molecular Weight Dependence of T-g Correlate to M-e? *Macromolecules* **2009**, *42* (7), 2877–2878.
- (70) Dollase, T.; Spiess, H. W.; Gottlieb, M.; Yerushalmi-Rozen, R. Crystallization of PDMS The effect of physical and chemical crosslinks. *Europhys. Lett.* **2002**, *60* (3), 390–396.
- (71) Allegra, G.; Ganazzoli, F. Configurations and Dynamics of Real Chains. 1. Polyethylene. *J. Chem. Phys.* **1981**, *74* (2), 1310–1320.
- (72) Perico, A.; Ganazzoli, F.; Allegra, G. A Hierarchy of Models for the Dynamics of Polymer-Chains in Dilute-Solution. *J. Chem. Phys.* **1987**, *87* (6), 3677–3686.
- (73) Dagger, A. C.; Arrighi, V.; Gagliardi, S.; Shenton, M. J.; Clarson, S. J.; Semlyen, J. A. Neutron scattering studies of cyclic and linear poly(dimethylsiloxanes). *ACS Sym Ser.* **2003**, *838*, 96–104.
- (74) Akcasu, A. Z.; Benmouna, M.; Han, C. C. Interpretation of Dynamic Scattering from Polymer-Solutions. *Polymer* **1980**, *21* (8), 866–890.
- (75) Bée, M. In *Quasielastic Neutron Scattering: Principles and Applications in Solid State Chemistry, Biology and Materials Science*; Hilger, A., Ed.; Bristol: Philadelphia, PA, 1988.
- (76) Chahid, A.; Alegria, A.; Colmenero, J. Methyl-Group Dynamics in Poly(Vinyl Methyl-Ether) - a Rotation Rate Distribution Model. *Macromolecules* **1994**, *27* (12), 3282–3288.
- (77) Frick, B.; Fetters, L. J. Methyl-Group Dynamics in Glassy Polyisoprene - a Neutron Backscattering Investigation. *Macromolecules* **1994**, *27* (4), 974–980.
- (78) Ngai, K. L.; Colmenero, J.; Alegria, A.; Arbe, A. Interpretation of Anomalous Momentum-Transfer Dependences of Local Chain Motion of Polymers Observed by Quasi-Elastic Incoherent Neutron-Scattering Experiments. *Macromolecules* **1992**, *25* (24), 6727–6729.
- (79) Colmenero, J.; Alegria, A.; Alberdi, J. M.; Alvarez, F.; Frick, B. Dynamics of the Alpha-Relaxation of A Glass-Forming Polymeric System - Dielectric, Mechanical, NMR, and Neutron-Scattering Studies. *Phys. Rev. B: Condens. Matter Mater. Phys.* **1991**, *44* (14), 7321–7329.
- (80) Alvarez, F.; Arbe, A.; Colmenero, J. Methyl group dynamics above the glass transition temperature: a molecular dynamics simulation in polyisoprene. *Chem. Phys.* **2000**, *261* (1–2), 47–59.
- (81) Frick, B.; Dosseh, G.; Cailliaux, A.; Alba-Simionesco, C. Pressure dependence of the segmental relaxation of polybutadiene and polyisobutylene and influence of molecular weight. *Chem. Phys.* **2003**, *292* (2–3), 311–323.
- (82) Bras, A. R.; Goossen, S.; Krutyeva, M.; Radulescu, A.; Farago, B.; Allgaier, J.; Pyckhout-Hintzen, W.; Wischniewski, A.; Richter, D. Compact structure and non-Gaussian dynamics of ring polymer melts. *Soft Matter* **2014**, *10* (20), 3649–3655.
- (83) Semlyen, J. A. Introduction: Cyclic Polymers - The First 40 Years. In *Cyclic Polymers*; Semlyen, J. A., Ed.; Springer Netherlands: Dordrecht, 2002; pp 1–46.
- (84) Tsalikis, D. G.; Koukoulas, T.; Mavrantzas, V. G.; Pasquino, R.; Vlassopoulos, D.; Pyckhout-Hintzen, W.; Wischniewski, A.; Monkenbusch, M.; Richter, D. Microscopic Structure, Conformation, and Dynamics of Ring and Linear Poly(ethylene oxide) Melts from Detailed Atomistic Molecular Dynamics Simulations: Dependence on Chain Length and Direct Comparison with Experimental Data. *Macromolecules* **2017**, *50* (6), 2565–2584.
- (85) Ozisik, R.; von Meerwall, E. D.; Mattice, W. L. Comparison of the diffusion coefficients of linear and cyclic alkanes. *Polymer* **2002**, *43* (2), 629–635.